Metabolism Clinical and Experimental 98 (2019) 62–75

Contents lists available at ScienceDirect

Metabolism Clinical and Experimental

journal homepage: www.metabolismjournal.com

PPP1R3C mediates metformin-inhibited hepatic gluconeogenesis

Xueying Ji [a,1], Shushu Wang [a,1], Hongju Tang [a,b,1], Yuqing Zhang [a], Feiye Zhou [a], Linlin Zhang [a], Qin Zhu [a], Kecheng Zhu [a], Qianqian Liu [a], Yun Liu [a], Xiao Wang [a,*], Libin Zhou [a,*]

[a] Shanghai Institute of Endocrine and Metabolic Diseases, Department of Endocrine and Metabolic Diseases, Shanghai Clinical Center for Endocrine and Metabolic Diseases, Ruijin Hospital, Shanghai Jiaotong University School of Medicine, Shanghai 200025, PR China
[b] The Department of Geriatrics, The People's of Wenshan Prefecture, Wenshan 663099, PR China

ARTICLE INFO

Article history:
Received 28 February 2019
Accepted 5 June 2019

Keywords:
PPP1R3C
Metformin
Gluconeogenesis
AMPK
TORC2
Liver

ABSTRACT

Background: Metformin has been widely used to alleviate hyperglycemia in patients with type 2 diabetes mainly *via* suppressing hepatic gluconeogenesis. However, the underlying mechanism remains incompletely clear. Here, we aimed to explore the role of PPP1R3C in metformin-mediated inhibition of hepatic gluconeogenesis.
Methods: The differentially expressed genes in primary mouse hepatocytes incubated with 8-Br-cAMP and metformin were analyzed by microarrays. Hepatic glucose production and gluconeogenic gene expressions were detected after adenovirus-mediated overexpression or silence of PPP1R3C *in vitro* and *in vivo*. The phosphorylation level and location of transducer of regulated CREB activity 2 (TORC2) were determined by Western blot and immunofluorescence.
Results: Metformin and adenovirus-mediated activation of AMPK suppressed 8-Br-cAMP–stimulated *Ppp1r3c* mRNA expression in primary mouse hepatocytes. Overexpression of PPP1R3C in primary mouse hepatocytes or the livers of wild-type mice promoted hepatic glucose production and gluconeogenic gene expressions. On the contrary, adenovirus-mediated knockdown of PPP1R3C in primary mouse hepatocytes decreased hepatic gluconeogenesis, with the suppression of cAMP-stimulated gluconeogenic gene expressions and TORC2 dephosphorylation. Notably, *Ppp1r3c* expression was increased in the liver of *db*/*db* mice. After PPP1R3C silence in the livers of wild-type and *db*/*db* mice, blood glucose levels and hepatic glucose production were markedly lowered, with decreased expressions of key gluconeogenic enzymes and transcript factors as well as liver glycogen content.
Conclusion: Metformin-activated AMPK decreases hepatic PPP1R3C expression, leading to the suppression of hepatic gluconeogenesis through blocking cAMP-stimulated TORC2 dephosphorylation. Hepatic specific silence of PPP1R3C provides a promising therapeutic strategy for type 2 diabetes.

1. Introduction

Inappropriate hepatic glucose production is the major cause of hyperglycemia in type 2 diabetic patients [1]. Metformin has been widely accepted as the first-line therapy of choice for patients with type 2 diabetes for several decades [2]. The major effect of metformin is to reduce hepatic glucose output *via* inhibiting gluconeogenesis [3,4], but the mechanism of its hypoglycemic action remains imperfectly understood.

At the cellular level, metformin is believed to disrupt hepatic gluconeogenesis process by antagonizing the glucagon signaling pathways *via* decreasing production of cyclic adenosine monophosphate (cAMP) or activating AMP-activated protein kinase (AMPK) [5–8]. AMPK, a well-known Serine/Threonine (Ser/Thr) kinase, functions as an intracellular energy sensor activated by an increase in the AMP/ATP ratio [9,10]. Once activated by metformin, AMPK inhibits the expressions of two rate-limiting gluconeogenic enzyme genes, phosphoenolpyruvate carboxykinase (PEPCK, encoded by *Pck1*) and glucose-6-phosphatase (G6Pase, encoded by *G6pc*), leading to a decrease in gluconeogenesis [11,12]. Although metformin is widely used as an AMPK agonist in biochemical studies, whether AMPK is actually the key effector of metformin on glucose metabolism is uncertain. It was shown that metformin blocked glucose production in mouse primary hepatocytes lacking all AMPK catalytic subunits [13].

Abbreviations: cAMP, Cyclic adenosine monophosphate; CREB, cAMP response element binding protein; PKA, Protein kinase A; TORC2, Transducer of regulated CREB activity 2; AMPK, AMP-activated protein kinase; PEPCK, Phosphoenolpyruvate carboxykinase; G6Pase, Glucose-6-phosphatase; PPP1R3C, Protein phosphatase 1 regulatory subunit G; 8-Br-cAMP, 8-Bromoadenosine 3′,5′-cyclic monophosphate; PTT, Pyruvate tolerance test; Fbpase, Fructose 1,6-bisphosphatase; SIK2, Salt inducible kinase 2.

* Corresponding authors at: Shanghai Institute of Endocrine and Metabolic Diseases, Department of Endocrine and Metabolic Diseases, Shanghai Clinical Center for Endocrine and Metabolic Diseases, Ruijin Hospital, Shanghai Jiaotong University School of Medicine, 197 Ruijin 2nd Road, Shanghai 200025, PR China.
E-mail addresses: wangxiao1976@hotmail.com (X. Wang), libinzhou99@hotmail.com (L. Zhou).
[1] These authors contributed equally to this study.

https://doi.org/10.1016/j.metabol.2019.06.002
0026-0495/

Pancreatic glucagon promotes hepatic gluconeogenesis by stimulating the protein kinase A (PKA)-mediated phosphorylation of cAMP response element binding protein (CREB) at Ser 133 and dephosphorylation of transducer of regulated CREB activity 2 (TORC2) at Ser 171 [14,15]. The subsequent recruitment of CREB-binding protein (CBP) leads to the formation of a CREB-CBP-TORC2 complex [16], which binds to an cAMP response element site (CRE) to increase transcription of peroxisome proliferator activated receptor γ coactivator-1α (PGC-1α), *Pck1*, and *G6pc* [17]. Increasing evidence suggests that TORC2 is the crucial factor in the regulation of glucose homeostasis and hepatic gluconeogenesis [18]. Metformin has been reported to stimulate the phosphorylation and nuclear exclusion of TORC2 [17]. However, the underlying molecular mechanism has not been fully elucidated.

The reversible phosphorylation of proteins is accomplished by the coordinated activation of Ser/Thr protein kinases and repression of counteracting phosphatases. Protein phosphatase 1 (PP1) consists of a catalytic subunit (PP1c) and a regulatory subunit (PP1r) [19]. There are seven genes (PPP1R3A to PPP1R3G) encoding PP1 regulatory subunit. As a glycogen-targeting regulatory subunit of PP1, PPP1R3C targets PP1 to glycogen, where it inhibits glycogen phosphorylase activity and activates glycogen synthase activity [20]. It has been demonstrated that overexpression of PPP1R3C in hepatocytes dramatically increases glycogen synthesis and storage [21,22] and might be involved in whole body energy metabolism [23]. However, little is known about the physiologic function of PPP1R3C upon hepatic gluconeogenesis. In the present study, PPP1R3C was identified as a potential target gene of metformin in suppressing cAMP-stimulated hepatic gluconeogenesis by microarray assay. Overexpression of PPP1R3C increased hepatic gluconeogenesis *in vitro* and *in vivo* while knockdown of PPP1R3C showed an opposite result. We further explored the molecular mechanism underlying PPP1R3C-regulated gluconeogenesis.

2. Materials and methods

2.1. Animal experiments

Male C57BL/6 mice aged 6–8 weeks were purchased from Shanghai Slack Experimental Center (Shanghai, China). Male *db*/*db* mice aged 4 weeks were purchased from Model Animal Research Center of Nanjing University (Nanjing, China). All mice were housed in temperature-controlled room (21 ± 1 °C) under a 12 h light/12 h dark cycle and given *ad libitum* access to a standard chow diet and tap water. All animal protocols were reviewed and approved by the Animal Care Committee of Ruijin Hospital, Shanghai Jiaotong University School of Medicine.

2.2. Isolation and culture of mouse primary hepatocyte

To isolate primary hepatocytes from male C57BL/6 mice aged 8 weeks, livers were perfused with 10 ml calcium-free HBSS (Sigma-Aldrich) followed by 20 ml liver digest media containing 0.05% collagenase IV (Gibco) through the portal vein in a recirculating manner for 15 min. Hepatocytes suspension was filtered through a 70 μm nylon mesh, centrifuged at 500*g* for 5 min at 4 °C, and washed three times with phosphate buffered solution (PBS). Isolated primary hepatocytes were incubated in hepatocyte medium containing 100 U/ml penicillin, 100 μg/ml streptomycin, 0.1% bovine *serum* albumin (BSA) and hepatocyte growth factor (ScienCell) at 37 °C in a 5% CO_2 humidified atmosphere.

2.3. Glucose production assay

For glucose production assay, hepatocytes were seeded (2.5×10^5 cells/well) in 24-well plates with pre-stimulation of DMEM containing 5.5 mM glucose, 0.25% BSA and 100 nM dexamethasone for 16 h. Next, cells were washed twice with PBS and incubated in glucose production buffer (DMEM without glucose, serum, and phenol red), supplemented with gluconeogenic substrates (10 mM sodium lactate and 1 mM pyruvate). After 8 h 8-Bromoadenosine 3′,5′-cyclic monophosphate (8-Br-cAMP) (Sigma-Aldrich) or metformin treatment, glucose concentrations in the media were determined by a commercially available glucose assay kit (Applygen).

2.4. Microarray analysis

Total RNA was extracted from isolated primary mouse hepatocytes incubated with 100 μM 8-Br-cAMP in the presence or absence of 2 mM metformin for 8 h using TRIzol (Thermo Fisher Scientific). Sample labeling and array hybridization were performed according to the Agilent One-Color Microarray-Based Gene Expression Analysis protocol (Agilent Technology) with minor modifications. The arrays were scanned by the Agilent Scanner G2505C. Agilent Feature Extraction software (version 11.0.1.1) was used to analyze the acquired array images. Quantile normalization and subsequent data processing were performed using the GeneSpring GX v12.0 software package (Agilent Technologies). Differentially expressed mRNAs between two groups were identified through Volcano Plot filtering (Fold Change ≥ 1.5, P value < 0.01). Gene Set Enrichment Analysis (GSEA) is supported by the Broad Institute website (http://www.broadinstitute.org/gsea/index.jsp) [24] and performed using the Java GSEA implementation.

2.5. Generation of recombinant adenoviruses

For overexpression, adenoviruses expressing mouse Ppp1r3c (Ad-Ppp1r3c), Creb (Ad-Creb) or green fluorescent protein (Ad-GFP) were constructed with a full-length Ppp1r3c, Creb or GFP cDNA coding sequence. To knockdown Ppp1r3c expression in hepatocytes, adenoviruses carrying short hairpin (sh) RNA targeting Ppp1r3c (shPpp1r3c-34: 5′-AAGTGAAGAATGTGAGCTT-3′; shPpp1r3c-35: 5′-CCTCCTATCGA TGAGTTAG-3′; shPpp1r3c-36:5′-CATTTCTTATCACGCTAAT-3′) or a scrambled sequence (shCtrl) were generated. Adenoviruses encoding full length mouse dominant-negative AMPK protein [AMPK-DN (D157A)] and a constitutively active form of AMPK [AMPK-CA(α-312)] were constructed. All recombinant adenoviruses were generated by GeneChem (Shanghai, China).

2.6. Adenovirus infection

Mouse primary hepatocytes were infected with adenovirus according to manufacturer instructions (GeneChem) for 24 h. For co-infection experiments, 24 h after infection with AMPK-CA, AMPK-DN or Ad-Creb, cells were coinfected with Ad-Ppp1r3c, Ad-GFP, shPpp1r3c or shCtrl for another 24 h. Cells were then performed further experiments.

2.7. Pyruvate tolerance test

Mice were injected through the tail vein with Ad-GFP, Ad-Ppp1r3c, shCtrl or shPpp1r3c (2×10^9 active viral particles in 200 μl saline). At 7 days after infection, pyruvate tolerance test (PTT) was performed by intraperitoneal injection of sodium pyruvate (Sigma-Aldrich) at a dose of 2 g/kg body weight after a 16 h fasting. Blood glucose was determined using a portable blood glucose meter (Lifescan, Johnson &Johnson). At 9 days after infection, mice were fasted for 16 h and then killed. Their livers and plasma were collected for further analysis.

2.8. Liver glycogen assay

The hepatic glycogen contents were measured by a commercial liver glycogen assay kit (Nanjing Jiancheng Bioengineering Institute) according to the manufacturer's protocols by colorimetric methods. After the reaction, the optical density (OD) value of glycogen suspension was

determined at 620 nm by spectrophotometer (Evolution 220, Thermo Fisher Scientific).

2.9. Reverse transcription-quantitative (RT-q) PCR

Total RNA was extracted from primary hepatocytes and mice livers using TRIzol reagent (Invitrogen) and reverse transcribed into cDNA using Random Primers (Promega) according to the manufacturer's protocol. RT-qPCR was performed in a Roche LightCycler 480 system (Roche Diagnostics) with SYBR Premix EX Taq (Takara). The primer sequences used for real-time PCR were shown in Table S1. Relative gene expression levels were quantified based on the cycle threshold (Cq) values and normalized to β-actin. The relative gene expression was calculated using the $2^{-\Delta\Delta Cq}$ method.

2.10. Western blot

Hepatic tissues or primary hepatocytes were lysed in radioimmunoprecipitation (RIPA) buffer containing protease inhibitor (Sigma-Aldrich) and centrifuged at 6000*g* at 4 °C for 10 min. Protein concentration was measured with a BCA protein assay kit (Thermo Fisher Scientific). Antibodies were purchased as following: anti-PPP1R3C antibody (GeneChem), anti-TORC2 antibody (Calbiochem), anti-p-AMPKα (Thr172) antibody (Cell Signaling), anti-t-AMPKα antibody (Cell Signaling), anti-acetyl-CoA carboxylase (ACC) antibody(Cell Signaling), anti-p-ACC (Ser79) antibody (Cell Signaling), anti-p-CREB (Ser133) antibody (Cell Signaling), anti-t-CREB antibody (Cell Signaling), Anti-PCK1 antibody (Abcam), anti-G6Pase antibody (Abcam), anti-GAPDH (HRP Conjugate) antibody (Cell Signaling), anti-HSP90 antibody (Cell Signaling), anti-α-Tubulin antibody (Abcam). The results were visualized using a chemiluminescence detection system (ImageQuant LAS 4000, GE Healthcare Life Science).

2.11. Immunofluorescence staining

Mice primary hepatocytes grown on collagen-coated cover slips were fixed for 20 min in PBS containing 4% paraformaldehyde, permeabilized in 0.1% Triton X100 for 5 min, and blocked in 5% (wt/vol.) BSA for 1 h. Cells were then incubated overnight 4 °C with rabbit anti-TORC2 antibody (1:200) and stained with FITC-labeled anti–guinea pig IgG (1:200, Jackson ImmunoResearch Laboratories). 4′,6-diamidino-2-phenylindole (DAPI) was added to stain cell nuclei. The cellular localization of TORC2 was photographed and analyzed by using a fluorescence microscope (Olympus BX51, Olympus).

2.12. Statistical analysis

All values are expressed as the mean ± standard error of the mean from at least three independent experiments. Comparisons were performed by using ANOVA for multiple groups or the Student's *t*-test for 2 groups. $P < 0.05$ was considered to indicate a statistically significant difference.

3. Results

3.1. Metformin reduces hepatic glucose production and gluconeogenic gene expression in isolated mouse hepatocytes

To investigate the effect of metformin on hepatic gluconeogenesis, 8-Br-cAMP (an *analogue* of *cAMP*) was used to mimic glucagon-elicited effect in hepatocytes. After primary mouse hepatocytes were incubated with 100 μM 8-Br-cAMP and various concentrations of metformin for 8 h, metformin dose-dependently suppressed 8-Br-cAMP-stimulated hepatic glucose production, with the maximum effect at the concentration of 2 mM (Fig. 1A). Treatment with 2 mM metformin led to a time-dependent inhibition on hepatic glucose production, with a significant effect at 4 h (Fig. 1B). According to the above results, the condition under 2 mM metformin treatment for 8 h was selected for the further experiments. Consistent with the results of hepatic gluconeogenesis, mRNA expressions of *Pck1*, *G6pc*, and fructose 1,6-bisphosphatase (Fbpase, encoded by *Fbp1*), three rate limiting enzymes of gluconeogenesis, were strongly induced by 8-Br-cAMP, which were dramatically decreased by metformin (Fig. 1C–E). Western blotting showed a similar result for PEPCK protein expression (Fig. 1F). Apparently, it is a well-established experiment condition for exploring the molecular mechanism underlying metformin-inhibited hepatic gluconeogenesis.

3.2. Ppp1r3c is a potential target gene of metformin in suppressing gluconeogenesis

To identify the target genes of metformin, the global gene expression patterns were analyzed in primary mouse hepatocytes exposed to 100 μM 8-Br-cAMP and 2 mM metformin for 8 h. By setting a threshold for differential expression at fold-change ≥1.5-fold, there were 1171 differentially expressed genes (642 upregulated and 529 downregulated genes) between 8-Br-cAMP-treated and control cells (Fig. 2A). Compared with 8-Br-cAMP group, 6072 differentially expressed genes (3515 upregulated and 2557 downregulated genes) were identified in metformin group (Fig. 2A). Among 642 cAMP-upregulated genes, 374 were downregulated by metformin (Fig. 2B). Of the 374 differentially expressed genes, 23 had been demonstrated to be associated with hepatic gluconeogenesis through consulting literature data, including classical gluconeogenic genes *Pck1*, *G6pc*, and *Fbp1*(Table S2). It is possible that other genes in this set of genes are also involved in the regulation of gluconeogenesis. Therefore, the 374 differentially expressed genes were further subjected to GO enrichment analysis, KEGG pathway analysis, and GSEA. GO enrichment analysis revealed that the cluster of genes were enriched in binding, catalytic activity, intercellular part, and metabolic process (Fig. 2C). The KEGG pathway enrichment analysis showed that the gluconeogenesis pathway was one of the most enriched pathways in the set of genes (Fig. 2D). By using GSEA, 9 differentially expressed genes between cAMP group and control group were core enrichment in gluconeogenesis pathways and the top-ranked gene was *Pck1* (Fig. 2E). In the set of genes enriched in cAMP + metformin group, GSEA identified 20 pathways associated with cellular response to metformin. The top-ranked pathway was the insulin-signaling pathway (Table S3). A ranked gene list of the insulin-signaling pathway was revealed, beginning with the most downregulated gene in cAMP + metformin group compared to cAMP group (Fig. 2F, Table S4). Interestingly, the top 5 enriched genes from this pathway all were involved in the regulation of protein phosphorylation, especially protein phosphatase 1, regulatory subunit 3B (*Ppp1r3b*/G_L/*PTG*), Protein phosphatase 1, regulatory subunit 3C (*Ppp1r3c*/*Ppp1r5*/*PTG*), and Phosphorylase kinase alpha 1 (*Phka1*). Both *Ppp1r3b* and *Ppp1r3c* are the regulatory subunits of PP1. PP1 catalyzes reversible protein dephosphorylation, which is important in a wide range of cellular function [19]. We further checked their fold changes in volcano plots and *Ppp1r3c* exhibited the most notable change among them, with 44.7-fold upregulation by 8-Br-cAMP and 39-fold downregulation by metformin (Fig. 2G). It is widely recognized that PPP1R3C exerts an important effect on glycogen metabolism [22,23,25]. Considering the remarkable changes of *Ppp1r3c* expression level in mouse hepatocytes in response to 8-Br-cAMP and metformin, it is reasonable to suppose that *Ppp1r3c* is involved in metformin-suppressed gluconeogenesis.

3.3. Metformin suppresses Ppp1r3c expression via AMPK-dependent pathway

We further characterized the effect of metformin on *Ppp1r3c* mRNA expression in mouse hepatocytes by RT-qPCR. 8-Br-cAMP-stimulated *Ppp1r3c* mRNA expression was gradually decreased with increased

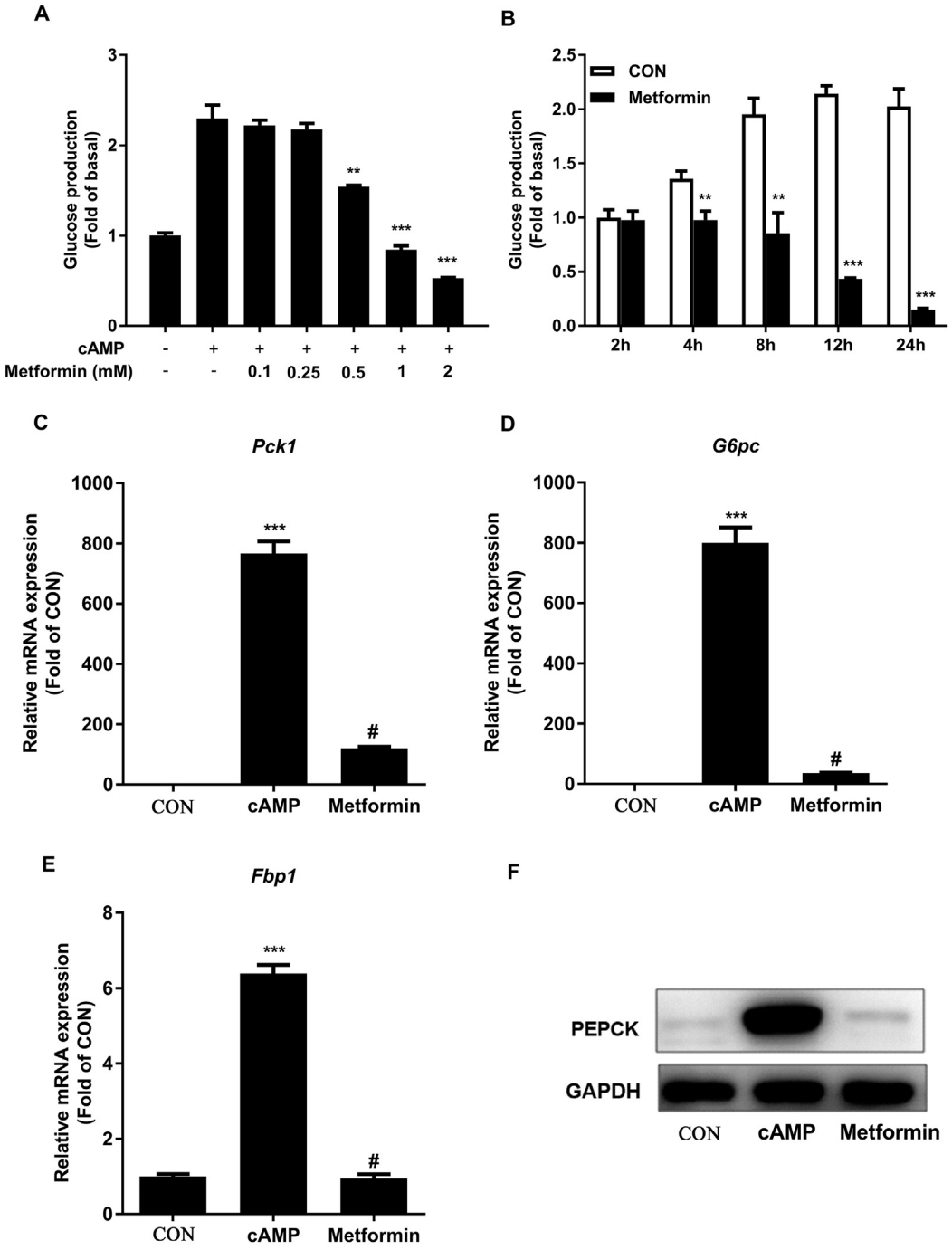

Fig. 1. Metformin inhibits cAMP-stimulated glucose production and gluconeogenic gene expressions in isolated mouse hepatocytes. (A) After isolated mouse hepatocytes were treated with 100 μM 8-Br-cAMP and various concentrations of metformin for 8 h, supernatant was taken for glucose production assay. $^{**}P < 0.01$, $^{***}P < 0.001$ *vs* cAMP alone. (B) After isolated mouse hepatocytes were treated with 100 μM 8-Br-cAMP and 2 mM metformin for the indicated time, supernatant was taken for glucose production assay. $^{**}P < 0.01$, $^{***}P < 0.001$ *vs* cAMP alone (CON). (C-E) RT-qPCR analysis of *Pck1*, *G6pc* and *Fbp1* mRNA expressions in mouse hepatocytes incubated with 100 μM 8-Br-cAMP and 2 mM metformin for 8 h. $^{***}P < 0.001$ *vs* control (CON); $^{\#}P < 0.05$ *vs* cAMP alone. (F) Protein level of PEPCK in mouse hepatocytes with 100 μM 8-Br-cAMP and 2 mM metformin for 12 h. Data are expressed as means ± SEM for 3 independent experiments.

concentrations of metformin (Fig. 3A). *Ppp1r3c* mRNA expression was significantly induced by 8-Br-cAMP at 4 h, and reached the peak at 8 h when the action of 8-Br-cAMP was completely reversed by 2 mM metformin (Fig. 3B). Like hepatic gluconeogenic genes including *Pgc1α*, *Pck1*, *G6pc*, and *Fbp1*, *Ppp1r3c* mRNA expression was upregulated by fasting in the liver of mice, and returned to basal level 2 h after refeeding (Fig. 3C). To investigate whether *Ppp1r3c* exerts an impact on hepatic gluconeogenesis, we transfected Ad-Ppp1r3c or shPpp1r3c into isolated mouse hepatocytes. After enforced expression of PPP1R3C in hepatocytes (Fig. 3D), hepatic glucose production was markedly enhanced in both basal and 8-Br-cAMP-stimulated statuses. Moreover, PPP1R3C overexpression antagonized metformin-suppressed gluconeogenesis (Fig. 3E). On the contrary, hepatic glucose production was significantly decreased in primary hepatocytes after Ppp1r3c was silenced (Fig. 3F and G).

There is a debate whether metformin-inhibited gluconeogenesis depends on AMPK activation [4,10,13]. In this current study, the phosphorylation levels of AMPK and its downstream substrate ACC were significantly increased by metformin in mouse hepatocytes, which was reversed by Compound C, an AMPK competitive inhibitor

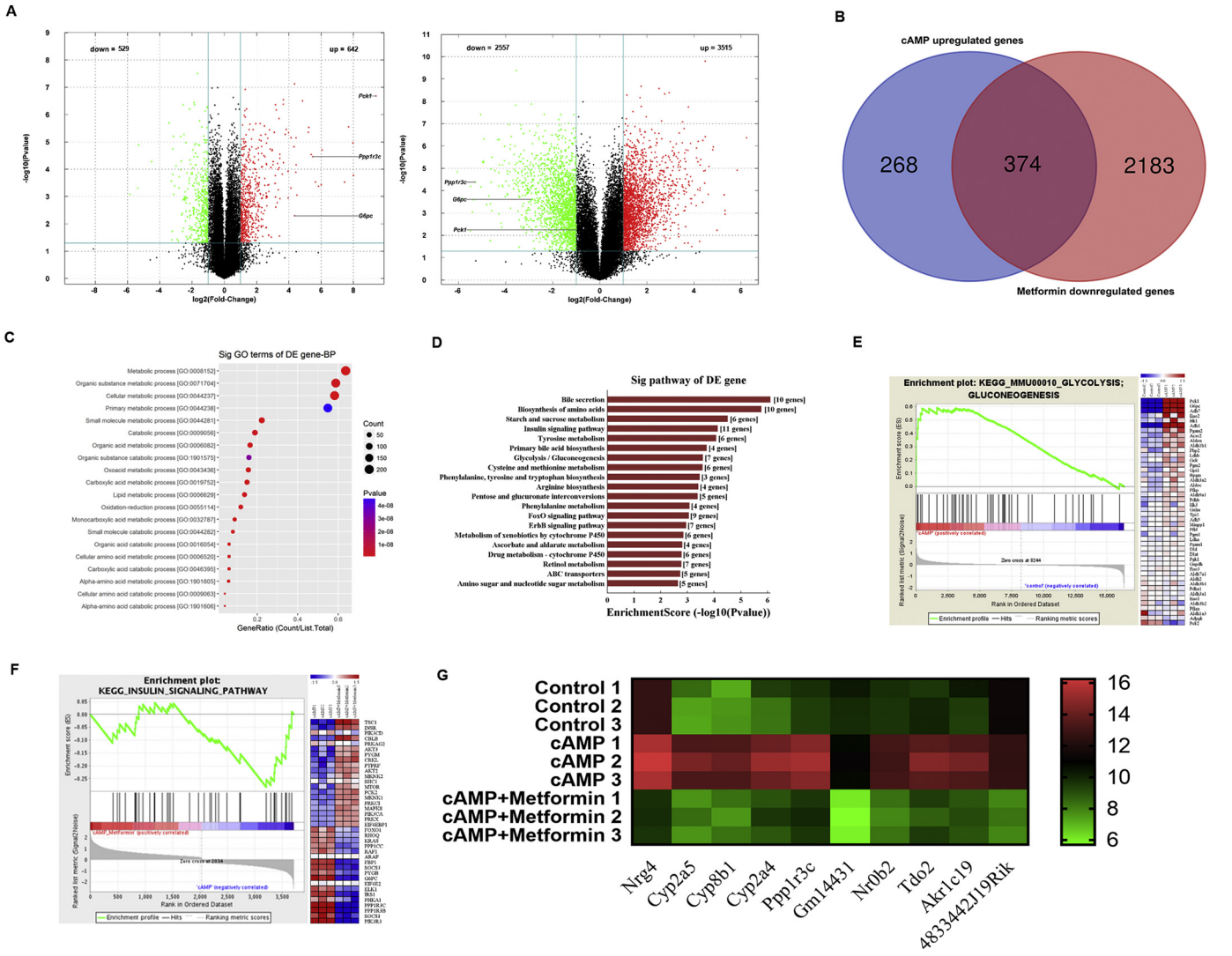

Fig. 2. Gene expression profiling of mouse hepatocytes in response to cAMP or metformin. Primary mouse hepatocytes treated with 100 μM 8-Br-cAMP in the presence or absence of 2 mM metformin for 8 h were used for microarray assay. (A) Volcano plots show the differentially expressed genes (Fold change > 1.5, $P < 0.01$) of cAMP group *vs* control group (left) and metformin group *vs* cAMP group (right). Red and green points indicate the upregulated and downregulated genes with statistical significance, respectively. (B) Venn diagrams of the differentially expressed genes (Fold change > 1.5, $P < 0.01$) upregulated by 8-Br-cAMP and downregulated by metformin. (C) The top 20 classifications associated with biological process according to GO annotations based on the 374 cAMP-upregulated genes reversed by metformin. (D) The top 20 most enriched pathways in KEGG pathway analysis. (E) Enrichment plot of Glycolysis/Gluconeogenesis pathway in GSEA analysis. (F) Enrichment plot of insulin signaling pathway in GSEA analysis. (G) Heat maps show the top 10 among 374 differentially expressed genes upregulated by 8-Brome-cAMP and reversed by metformin. Three independent experiments were performed for each group.

(Fig. 4A). Meanwhile, Compound C antagonized the inhibitory effect of metformin on hepatic glucose production (Fig. 4B). To exclude the non-specific action of Compound C, AMPK-DN or AMPK-CA adenovirus was transfected into mouse hepatocytes. Metformin-suppressed hepatic gluconeogenesis was reversed by AMPK-DN (Fig. 4C) while AMPK-CA transfection completely abolished cAMP-induced gluconeogenesis in hepatocytes (Fig. 4D). Correspondingly, cAMP-stimulated mRNA expressions of *Pck1* and *G6pc* were significantly decreased by AMPK-CA transfection (Fig. 4E). The protein expressions of the two gluconeogenic genes showed a similar result under the same condition (Fig. 4F). These results indicate that the inhibitory effect of metformin on hepatic gluconeogenesis relies on the activation of AMPK.

To determine whether *Ppp1r3c* is involved in AMPK activation-mediated regulation of gluconeogenesis, primary mouse hepatocytes were transfected with control or AMPK-CA adenoviruses. Not surprisingly, AMPK-CA abolished cAMP-stimulated *Ppp1r3c* mRNA expression as expected (Fig. 4G). Ppp1r3c overexpression antagonized AMPK-CA-suppressed hepatic gluconeogenesis induced by cAMP (Fig. 4H). Moreover, the stimulatory effect of AMPK-DN on gluconeogenesis was abrogated by Ppp1r3c knockdown (Fig. 4I). These results indicate that metformin decreased hepatic gluconeogenesis through AMPK activation-suppressed *Ppp1r3c* expression.

3.4. Ppp1r3c regulates TORC2 phosphorylation and nuclear translocation in mouse hepatocytes

It has been demonstrated that PKA-mediated phosphorylation of CREB and dephosphorylation of TORC2 is key to promote hepatic gluconeogenesis [16,17]. Our study showed that metformin blocked 8-Br-cAMP-stimulated TORC2 dephosphorylation in primary mouse hepatocytes, but without impact on CREB phosphorylation (Fig. 5A). Additionally, there existed an interaction of TORC2 with PP1 in mouse hepatocytes as shown in Fig. 5B. Since PP1 activity could be enhanced by overexpression of Ppp1r3c [26], it is likely that Ppp1r3c regulates TORC2 phosphorylation level *via* activating PP1. Sure enough, transfection with shPpp1r3c blocked the dephosphorylation of TORC2 elicited by 8-Br-cAMP, whereas no significant change was observed for the phosphorylation level of CREB (Fig. 5C). Furthermore,

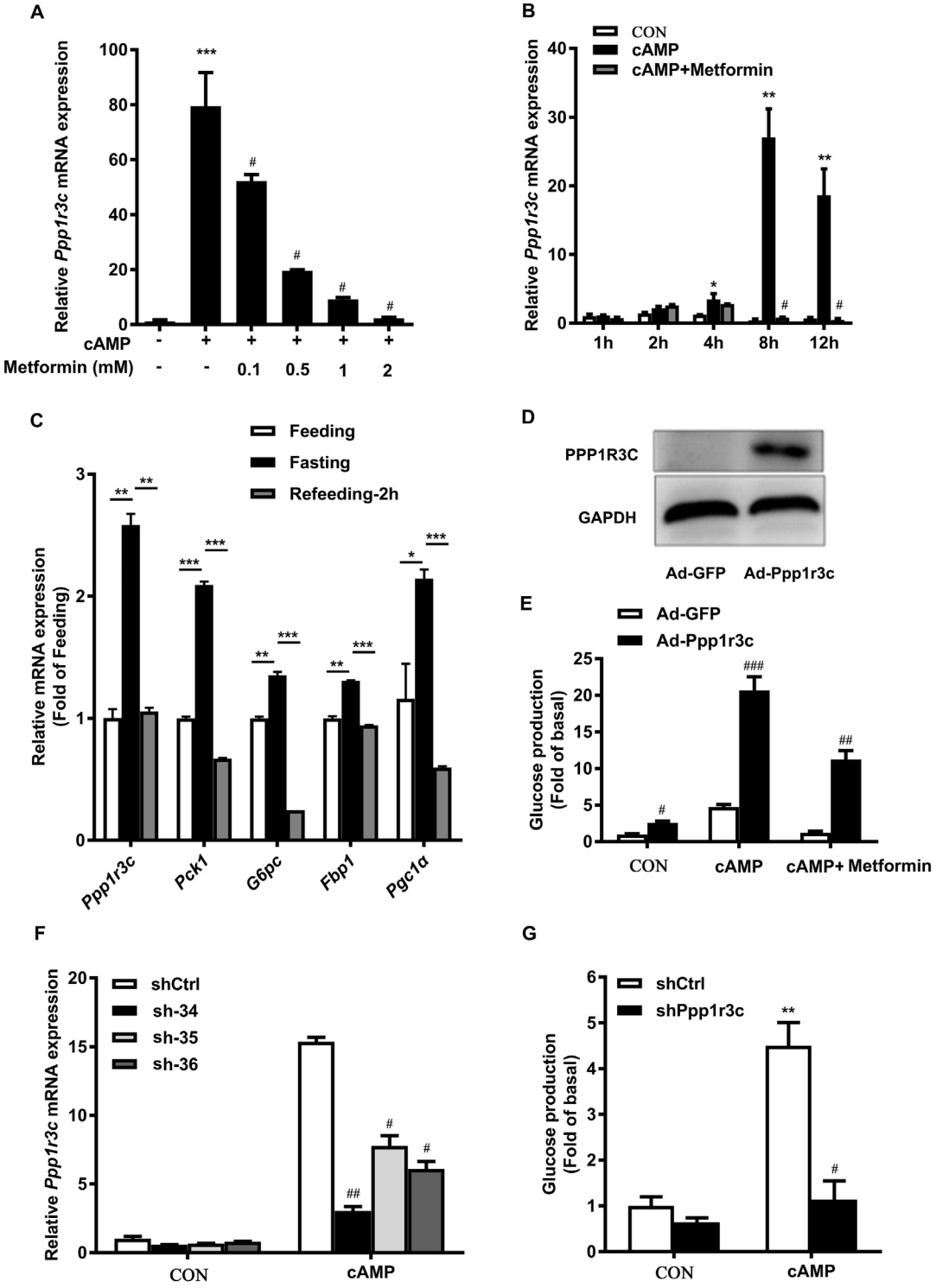

Fig. 3. PPP1R3C regulates hepatic glucose production in isolated mouse hepatocytes. (A) *Ppp1r3c* mRNA expression in isolated mouse hepatocytes incubated with 100 μM 8-Br-cAMP and various concentrations of metformin. (B) *Ppp1r3c* mRNA expression in isolated mouse hepatocytes incubated with 100 μM 8-Br-cAMP and 2 mM metformin for the indicated time. (C) The mRNA expression of *Ppp1r3c* and gluconeogenic genes in livers of C57BL/6 mice under fasting and refeeding conditions. (D) Protein level of PPP1R3C in mouse hepatocytes with Ad-Ppp1r3c or Ad-GFP transfection. (E) After mouse hepatocytes transfected with Ad-Ppp1r3c or Ad-GFP were incubated in 100 μM 8-Br-cAMP and 2 mM metformin for 8 h, hepatic glucose output was assayed. (F) Mouse hepatocytes were transfected with three shRNAs for Ppp1r3c (sh-34, sh-35, sh-36) and control shRNA (shCtrl) for 24 h and incubated with 100 μM 8-Br-cAMP for 8 h. *Ppp1r3c* mRNA was detected by RT-qPCR. (G) Mouse hepatocytes infected with shCtrl and shPpp1r3c were incubated with 100 μM 8-Br-cAMP and 2 mM metformin for 8 h. Glucose content in culture medium was assayed. Data are expressed as means ± SEM for 3 independent experiments. $^{*}P < 0.05$, $^{**}P < 0.01$, $^{***}P < 0.001$ *vs* control (CON); $^{\#}P < 0.05$, $^{\#\#}P < 0.01$, $^{\#\#\#}P < 0.001$ *vs* cAMP alone, Ad-GFP, or shCtrl.

immunofluorescence staining exhibited a corresponding result. TORC2 was mainly localized in the cytoplasm of mouse hepatocytes at basal status, and Ppp1r3c knockdown remarkably limited TORC2 nuclear entry in hepatocytes in response to forskolin (Fig. 5D and E). After nuclear entry, dephosphorylated TORC2 is thought to stimulate gluconeogenic gene expression through an association with phosphorylated CREB [27]. Consistent with the result of disrupt TORC2 nuclear entry, 8-Br-cAMP-induced mRNA expressions of *Pck1*, *G6pc* and *Fbp1*

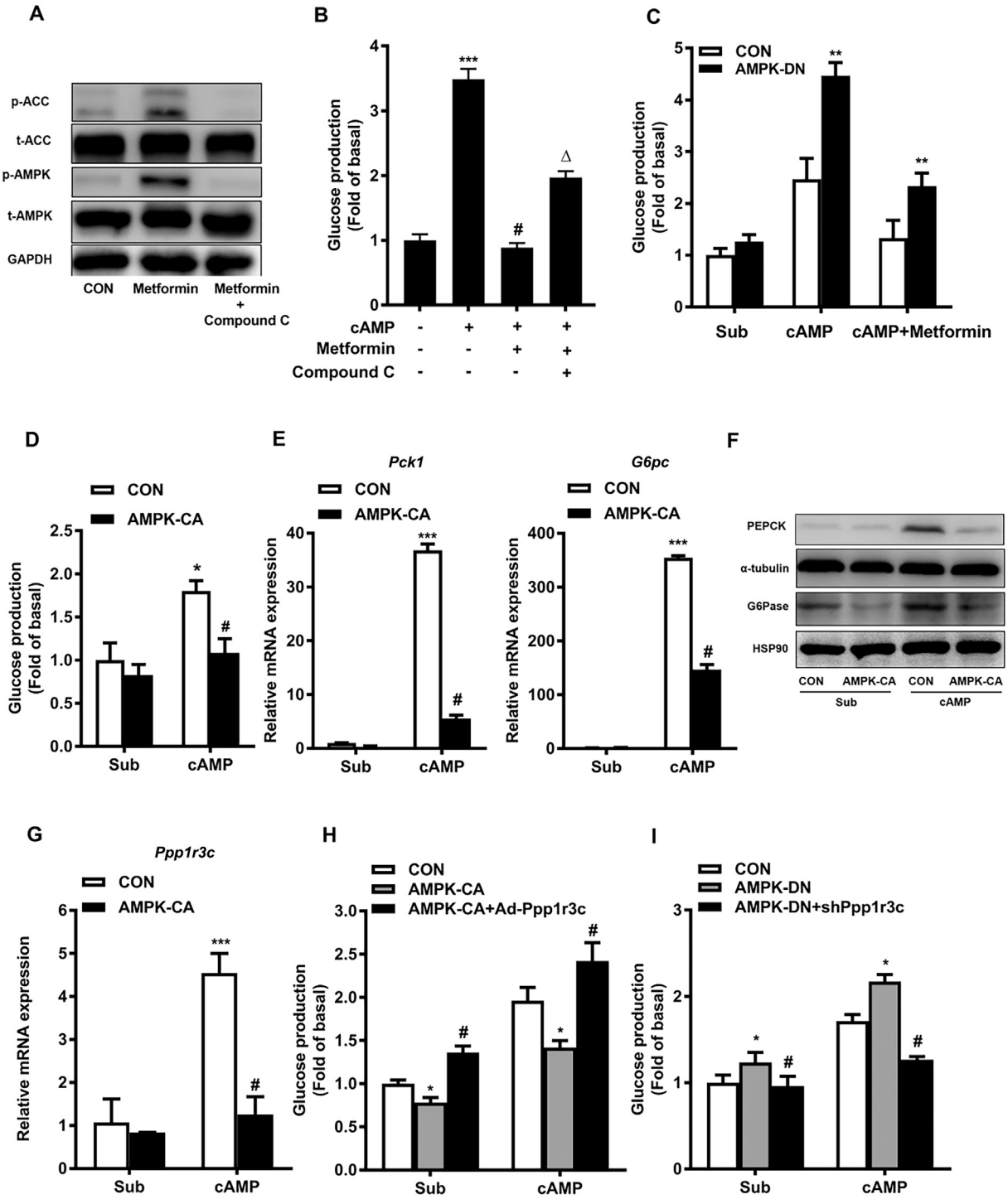

Fig. 4. AMPK activation decreases hepatic glucose production *via* suppressing PPP1R3C expression. (A) AMPK and ACC protein phosphorylation levels in mice hepatocytes treated with 2 mM metformin or 10 μM compound C. (B) Glucose production in mouse hepatocytes treated with 100 μM 8-Br-cAMP, 2 mM metformin or 10 μM compound C. $^{***}P < 0.001$ *vs* basal, $^{\#}P < 0.05$ *vs* cAMP alone, $^{\Delta}P < 0.05$ *vs* cAMP plus metformin. (C) Glucose production in mouse hepatocytes transfected with AMPK-DN. $^{**}P < 0.01$ *vs* control adenovirus (CON). After mouse hepatocytes transfected with AMPK-CA were incubated with 100 μM 8-Br-cAMP for 8 h or 12 h, glucose content levels were assayed (D), and PEPCK and G6Pase expression levels were detected by RT-qPCR (E) and Western blot (F). $^{*}P < 0.05$, $^{***}P < 0.001$ *vs* basal, $^{\#}P < 0.05$ *vs* control adenovirus. (G) Ppp1r3c mRNA expression in mouse hepatocytes transfected with AMPK-CA for 24 h and treated with 100 μM 8-Br-cAMP for 8 h. $^{***}P < 0.001$ *vs* basal, $^{\#}P < 0.05$ *vs* control adenovirus. (H) Glucose production in mouse hepatocytes co-transfected with Ad-Ppp1r3c and AMPK-CA and incubated with 100 μM 8-Br-cAMP. $^{*}P < 0.05$ *vs* control adenovirus (CON), $^{\#}P < 0.05$ *vs* AMPK-CA. (I) Glucose production in mouse hepatocytes co-transfected with shPpp1r3c and AMPK-DN and incubated with 100 μM 8-Br-cAMP. $^{*}P < 0.05$ *vs* control adenovirus (CON), $^{\#}P < 0.05$ *vs* AMPK-DN. Data are expressed as means ± SEM for 3 independent experiments.

were accordingly reduced by shPpp1r3c transfection (Fig. 5F). This was the case for PEPCK and G6Pase protein expressions (Fig. 5G). To investigate whether PPP1R3C affects CREB-initiated gluconeogenesis, primary mouse hepatocytes were co-transfection with Ad-Creb and shPpp1r3c adenoviruses. PPP1R3C knockdown inhibited CREB-elevated hepatic glucose production in the presence or absence of 8-Br-cAMP (Fig. 5H).

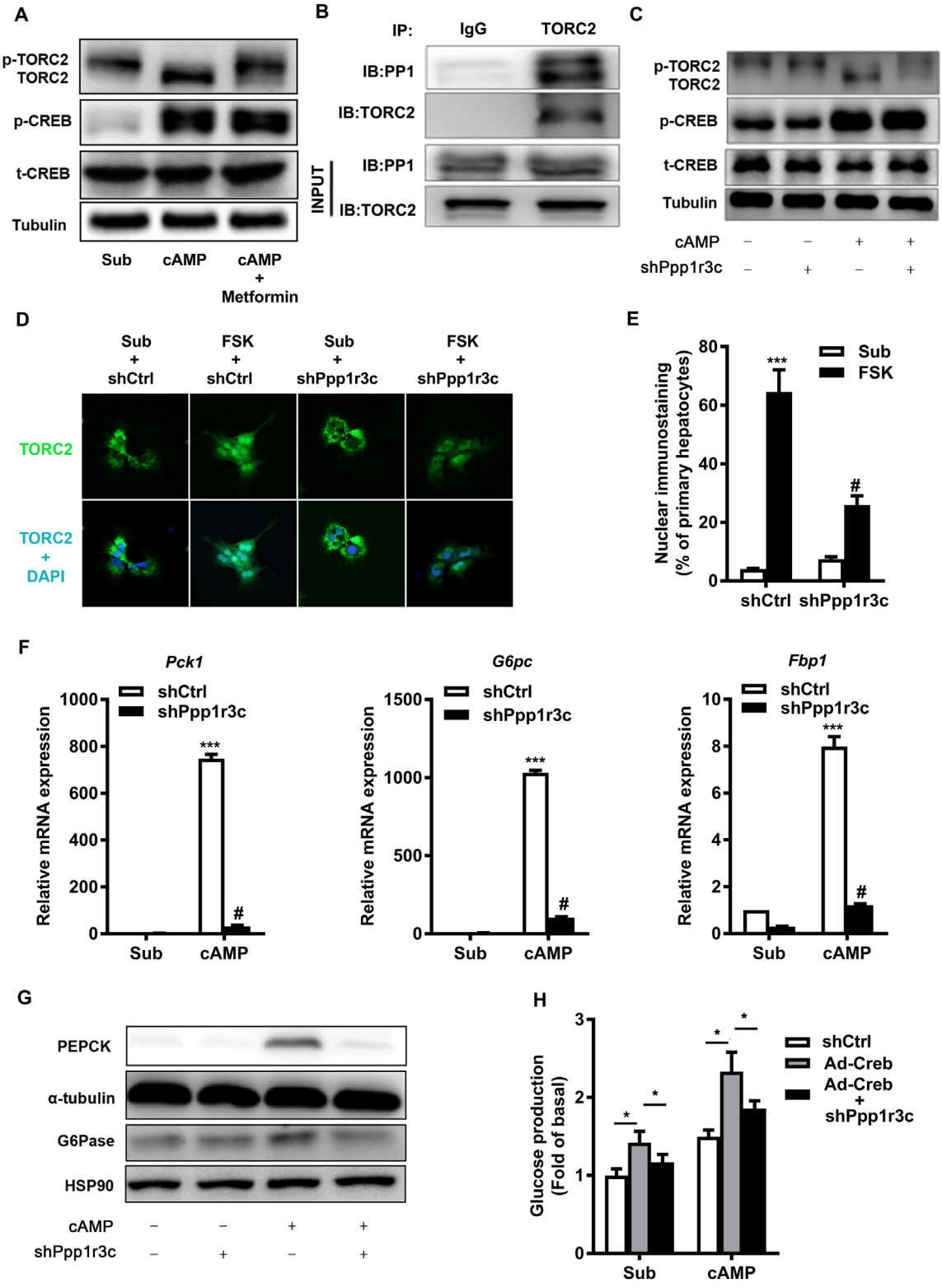

Fig. 5. PPP1R3C knockdown blocks cAMP-stimulated dephosphorylation of TORC2 in mouse primary hepatocytes. (A) TORC2 and CREB phosphorylation levels in mouse hepatocytes incubated with 100 μM 8-Br-cAMP and 2 mM metformin for 1 h. (B) Coimmunoprecipitation (CoIP) validated the interaction of PP1 and TORC2 in mouse hepatocytes. (C) Protein phosphorylation levels of TORC2 and CREB in mice hepatocytes transfected with shPpp1r3c or shCtrl for 24 h and incubated with 100 μM 8-Br-cAMP 1 h. (D) Immunofluorescence analysis of TORC2 localization in hepatocytes transfected with shPpp1r3c or shCtrl adenovirus for 24 h and incubated with 10 μM forskolin (FSK) for 1 h. (E) TORC2 nuclear staining percentage in mouse primary hepatocytes. (F) *Pck1*, *G6pc*, and *Fbp1* mRNA expressions in mouse hepatocytes transfected with shPpp1r3c or shCtrl for 24 h and incubated with 100 μM 8-Br-cAMP for 8 h. (G) Protein expressions of PEPCK and G6Pase in mouse hepatocytes transfected with shPpp1r3c or shCtrl for 24 h and incubated with 100 μM 8-Br-cAMP for 12 h. (H) Mouse hepatocytes co-transfected with Ad-Creb and shPpp1r3c were incubated with 100 μM 8-Br-cAMP for 8 h and glucose production was assayed. Data are expressed as means ± SEM for 3 independent experiments. $^{*}P < 0.05$, $^{***}P < 0.01$ *vs* basal, $^{\#}P < 0.05$ *vs* control adenovirus (shCtrl).

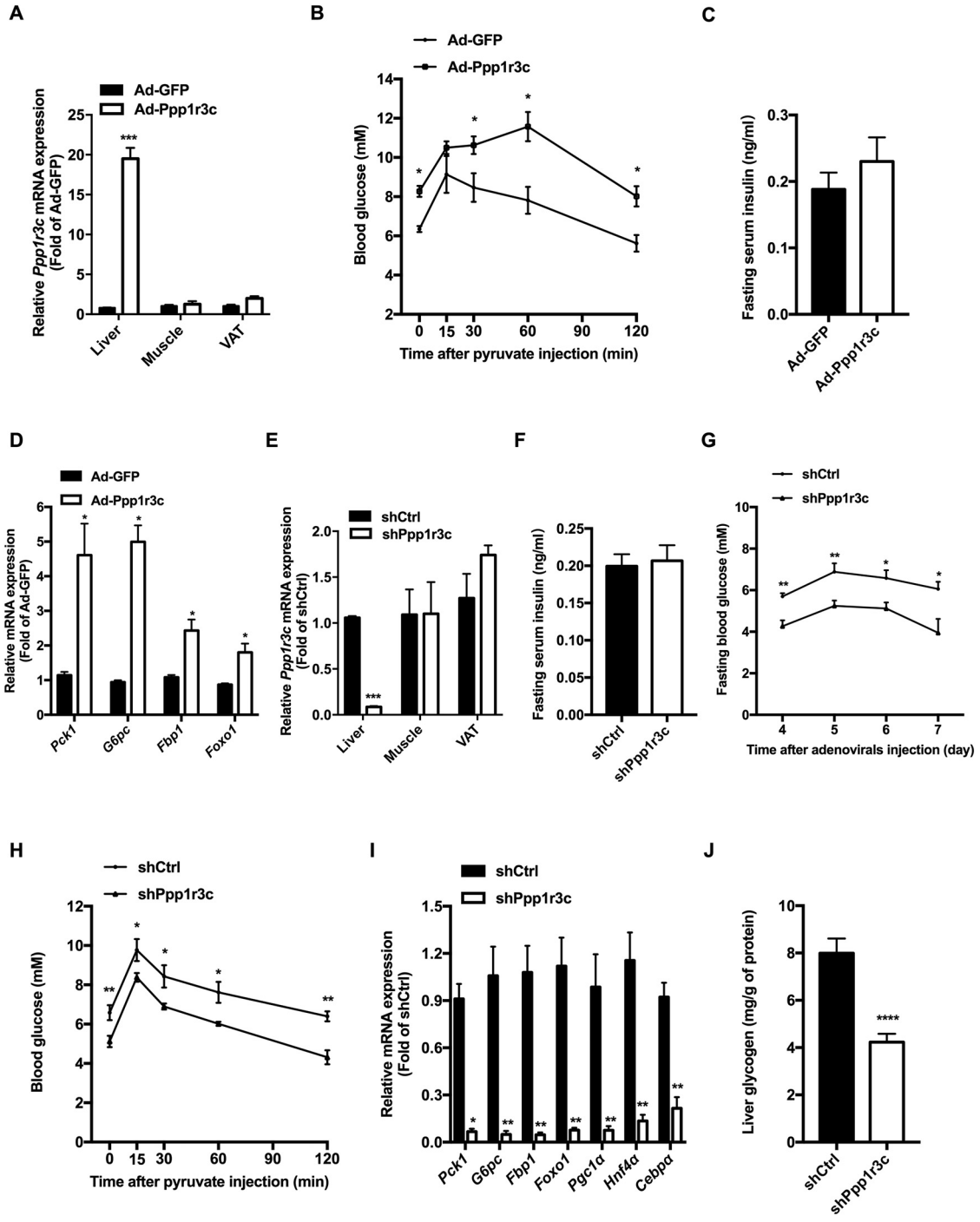

Fig. 6. Effect of PPP1R3C knockdown or overexpression on glucose metabolism in C57BL/6 mice. (A) *Ppp1r3c* mRNA expression in the liver, skeletal muscle, and visceral adipose tissues (VAT) of mice injected with Ad-Ppp1r3c or Ad-GFP adenoviral vectors. (B) PTT after 16 h fasting in mice injected with Ad-Ppp1r3c or Ad-GFP adenoviral vectors. (C) Fasting serum insulin in mice injected with Ad-Ppp1r3c or Ad-GFP adenoviral vectors. (D) Hepatic mRNA expressions of gluconeogenic genes in mice treated with Ad-Ppp1r3c or Ad-GFP. (E) *Ppp1r3c* mRNA expression in the liver, skeletal muscle, and VAT, (F) fasting serum insulin, (G) fasting blood glucose, (H) PTT, (I) gluconeogenic gene expressions, and (J) liver glycogen content in mice injected with shPpp1r3c or shCtrl adenovirus. PTT was performed 7 days after adenovirus injection and mice were killed 9 days after adenovirus injection. Data are expressed as means ± SEM ($n = 6$). $^{*}P < 0.05$, $^{**}P < 0.01$, $^{***}P < 0.001$ *vs* control mice.

Taken together, these results indicate that Ppp1r3c plays a regulatory role in hepatic gluconeogenesis through controlling TORC2 nuclear entry.

3.5. Metabolic effects of Ppp1r3c in normal wild-type mice

To investigate the *in vivo* effect of PPP1R3C on hepatic glucose production, Ad-Ppp1r3c was injected into wild-type C57BL/6 mice by tail vein and Ppp1r3c expression was significantly increased in liver, not in skeletal muscle and visceral adipose tissues (Fig. 6A). In PPP1R3C overexpressing mice, the blood glucose levels were significantly higher than those of control mice at 0, 30, 60, and 120 min during PTT (Fig. 6B), without significant changes of fasting serum insulin (Fig. 6C), alanine aminotransferase, aspartate aminotransferase levels (supplemental Fig. S1A and B), and body weight (not shown). In consistent with this result, the mRNA expressions of four gluconeogenic genes including *Pck1*, *G6pc*, *Fbp1*, and *Foxo1* were upregulated in the liver of Ad-Ppp1r3c transfected mice (Fig. 6D). On the contrary, after shPpp1r3c adenovirus

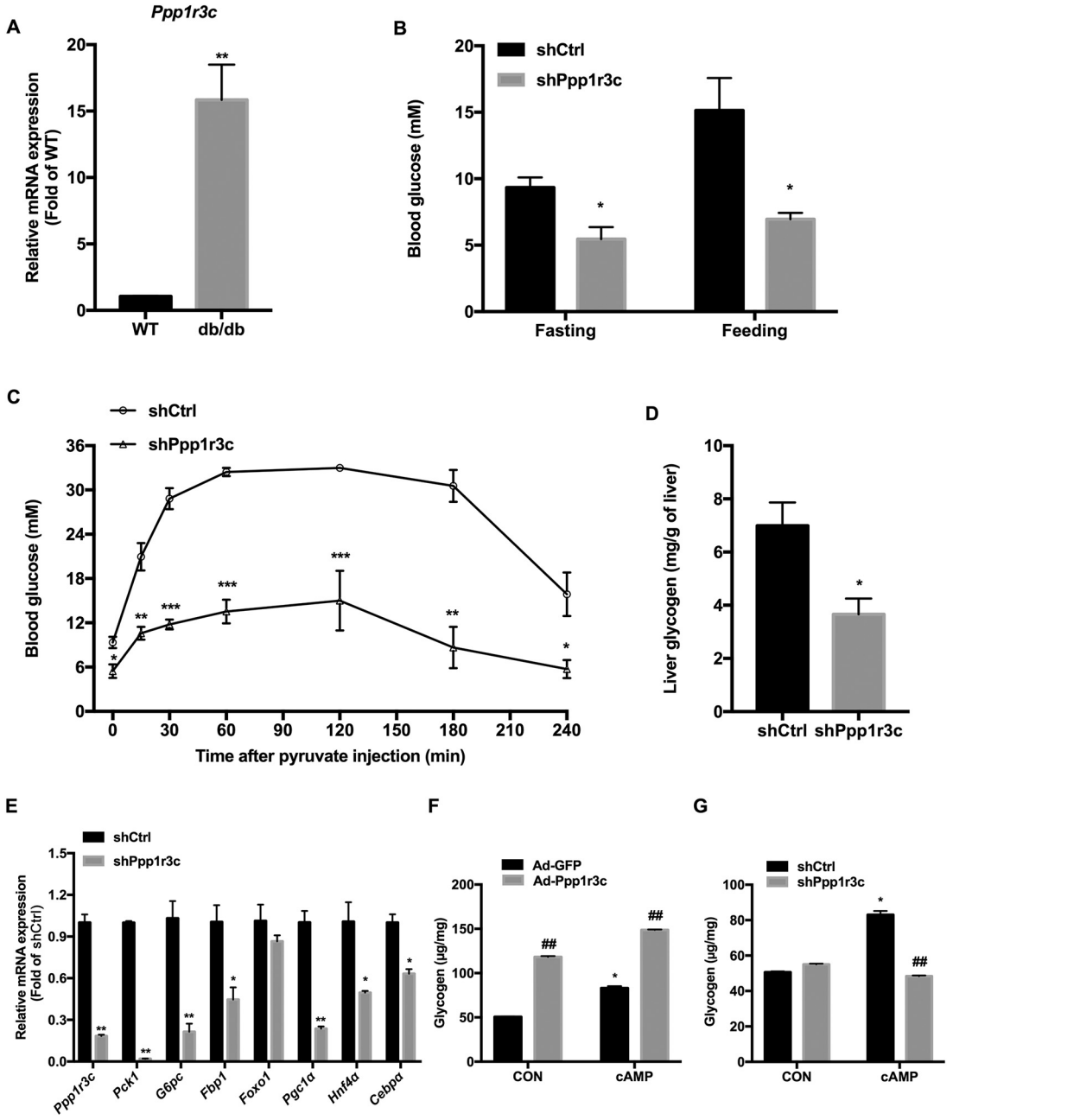

Fig. 7. PPP1R3C knockdown inhibits hepatic gluconeogenesis in *db/db* mice. (A) Hepatic mRNA expression of *Ppp1r3c* in WT mice and *db/db* mice. (B) Blood glucose levels, (C) PTT, (D) liver glycogen content, (E) hepatic mRNA expression of gluconeogenic genes in mice treated with shPpp1r3c or shCtrl. PTT was performed 7 days after adenovirus injection and mice were killed 9 days after adenovirus injection. Data are expressed as means ± SEM ($n = 5$). $^{*}P < 0.05$, $^{**}P < 0.01$, $^{***}P < 0.001$ *vs* control mice. Wild-type mouse hepatocytes infected with Ad-GFP and Ad-Ppp1r3c (F) or shCtrl and shPpp1r3c (G) were incubated with 100 μM 8-Br-cAMP for 8 h. Glycogen content in hepatocytes was assayed. $^{*}P < 0.05$, *vs* control (CON); $^{\#\#}P < 0.01$, *vs* Ad-GFP or shPpp1r3c.

was injected into wild-type C57BL/6 mice by tail vein and Ppp1r3c expression was dramatically decreased in liver, not in skeletal muscle and visceral adipose tissues (Fig. 6E). There were no obvious differences in fasting serum insulin (Fig. 6F), two liver enzyme levels (supplemental Fig. S1C and D), and body weight (not shown) between the two groups. Fasting blood glucose level was decreased in shPpp1r3c-treated mice compared with control mice (Fig. 6G). PTT revealed a significant decrease in hepatic glucose production in shPpp1r3c-treated mice, with lower blood glucose levels at all time points (Fig. 6H). The mRNA expressions of key gluconeogenic enzymes and transcription factors including Pck1, G6pc, Fbp1, Foxo1, Pgc1α, Hnf4α, and Cebpα were downregulated in the liver of shPpp1r3c-treated mice (Fig. 6I). In the liver tissue, knockdown of PPP1R3C reduced the glycogen content by nearly half (Fig. 6J).

3.6. Effects of Ppp1r3c knockdown on glucose metabolism in db/db mice

Interestingly, Ppp1r3c mRNA expression in the liver of *db/db* mice was markedly elevated compared with that in wild-type mice (Fig. 7A). To investigate the therapeutic potential of Ppp1r3c, we administered shPpp1r3c adenovirus to *db/db* mice by tail vein injection. shPpp1r3c-treated *db/db* mice showed lower fasting and nonfasting blood glucose levels compared with scramble shRNA-treated *db/db* mice (Fig. 7B). Similar to the findings in wild-type mice, shPpp1r3c

treatment considerably decreased blood glucose levels in *db*/*db* mice in the whole process of PTT (Fig. 7C). In parallel with the alleviated hyperglycemia in shPpp1r3c-treated mice, the hepatic expressions of genes related to gluconeogenesis were reduced to some extent (Fig. 7D). The glycogen content of liver was decreased by 47.7% in shPpp1r3c-treated *db*/*db* mice (Fig. 7E). We further investigated the effect of Ppp1r3c on glycogen synthesis in isolated mouse hepatocytes in glucose-free culture media containing sodium lactate and pyruvate. Overexpression of Ppp1r3c increased glycogen content under both basal and cAMP-stimulated conditions (Fig. 7F). Conversely, Ppp1r3c knockdown abolished cAMP-stimulated glycogen synthesis, without effect at basal status (Fig. 7G). These results suggest that Ppp1r3c is a double modulator of hepatic gluconeogenesis and glycogen synthesis.

4. Discussion

The liver plays a major role in the maintenance of normal glucose homeostasis by controlling the balance between hepatic glucose production and storage. During fasting, increased circulating glucagon triggers the gluconeogenic programme *via* activating the cAMP pathway [28]. In the present study, 8-Br-cAMP well mimicked the fasting action of glucagon as the expressions of three key gluconeogenic genes *Pck1, G6pc, and Fbp1* were strongly upregulated by it in the global gene expression profiles, with the most highly induced gene being Pck1. Coincidentally, the expressions of these three genes were dramatically decreased in the presence of metformin, exhibiting a high reliability for this set of microarray data. Therefore, we focused on the cluster of 8-Br-cAMP-upregulated and metformin-downregulated genes. It is well-known that protein phosphorylation plays a crucial role in the regulation of hepatic gluconeogenesis. The expression of PPP1R3C, a PP1 regulatory subunit, was paralleled with key gluconeogenic genes in primary hepatocytes incubated with 8-Br-cAMP and metformin as well as in the liver of fasting and feeding mice. Using PPP1R3C overexpressing or interfering adenovirus, we demonstrated a key role of PPP1R3C in the regulation of hepatic glucose production *in vitro* and *in vivo*.

Enhanced hepatic gluconeogenesis is a crucial contributor of hyperglycemia in type 2 diabetes [29]. Metformin alleviates hyperglycemia mainly *via* suppressing hepatic gluconeogenesis [30]. However, there exists a contradiction about whether AMPK is indispensable to the hypoglycemic effect of metformin. Metformin activates AMPK through inhibiting the mitochondrial respiratory chain complex I and increasing the cellular AMP:ATP ratio [31], which promotes AMPKα2 phosphorylation at Thr172 by the tumor suppressor Liver Kinase B1 (LKB1) [32]. Hepatic deletion of LKB1 abolished the hypoglycemic effects of metformin in high fat fed diabetic mice [4]. Knockout of AMPK catalytic α-subunits abrogated metformin-suppressed gluconeogenesis stimulated by cAMP or glucagon [33]. However, another study showed that metformin was still able to lower blood glucose level in liver AMPK-deficient mice and hepatic glucose production in primary hepatocytes from these mice [13]. In the present study, the metformin-mediated suppression of hepatic gluconeogenesis was attenuated in hepatocytes treated with compound C or AMPK-DN, supporting that the inhibitory effect of metformin on hepatic gluconeogenesis is at least partially attributed to AMPK activation.

TORC2 is a pivotal regulator of the gluconeogenic programme in response to both hormonal and intracellular signals [34]. Under *ad libitum* feeding conditions, TORC2 is sequestered in the cytoplasm through phosphorylation-dependent interactions with 14-3-3 proteins. In response to fasting, TORC2 is dephosphorylated and translocated to the nucleus where it mediates CREB-dependent transcription of Pgc-1α and its subsequent gluconeogenic target genes Pepck and G6Pase [17]. LKB1/AMPK signaling has been reported to regulate the phosphorylation and nuclear exclusion of TORC2. AICAR-activated AMPK and insulin-activated salt inducible kinase 2 (SIK2) are found to induce phosphorylation and nuclear export of TORC2 in hepatocytes [35,36]. In this current study, cAMP-elicited TORC2 dephosphorylation, not CREB phosphorylation was prevented by metformin in primary hepatocytes. Apparently, the block of TORC2 nuclear translocation is a crucial step for metformin-suppressed gluconeogenesis *via* activating AMPK. However, the mechanism underlying AMPK-stimulated TORC2 phosphorylation still remains unclear.

Noradrenaline was reported to stimulate Ppp1r3c mRNA expression *via* cAMP pathway in mouse cortical astrocytes [37]. Ppp1r3c mRNA levels were strongly upregulated in the process of 3T3-L1 adipocyte differentiation [26], which involves cAMP signal pathway. Foxa2, a transcriptional regulator of hepatic gluconeogenic genes [38], mediated cAMP-stimulated transcription of Ppp1r3c by binding to its promoter in liver cells [39]. Metformin inhibited FoxA2-induced G6Pase promoter activity [40]. In consistent with these results, our study also revealed a strong induction of Ppp1r3c by 8-Br-cAMP in mouse primary hepatocytes. The expressions of Ppp1r3c and gluconeogenic genes including Pgc1α, Pck1, G6pc, and Fbp1 were significantly up-regulated in liver of fasting mice and returned to normal after refeeding (Fig. 3C). Metformin treatment abrogated glucagon-stimulated cAMP accumulation *via* direct inhibition of adenylate cyclase, resulting in the suppression of the cAMP/PKA pathway and gluconeogenesis [7]. A recent study showed that AMPK activation antagonized glucagon-triggered cAMP/PKA signaling by activating cyclic nucleotide phosphodiesterase 4B in primary mouse hepatocytes [41]. In this study, metformin abolished 8-Br-cAMP-stimulated expression of Ppp1r3c. Silence of PPP1R3C abrogated 8-Br-cAMP-elevated hepatic glucose production in mouse hepatocytes, with decreased expressions of key gluconeogenic enzymes. Overexpression of PPP1R3C antagonized AMPK-CA- and metformin-mediated suppression of gluconeogenesis. Moreover, adenovirus-mediated activation of AMPK decreased 8-Br-cAMP-stimulated Ppp1r3c expression. These results suggest that metformin reduces hepatic gluconeogenesis *via* AMPK activation-inhibited Ppp1r3c expression. It has been demonstrated that hepatic TORC2 dephosphorylation and activation under fasting or insulin resistant condition are mediated by activated Ser/Thr phosphatases such as PP2A, PP2B or SMEK/PP4C [42–44]. PP1 exhibits a different role in cAMP-mediated gene expression through dephosphorylating CREB [42] and TORC2 [45]. Our Co-IP assay revealed an interaction of PP1 and TORC2. We further investigated whether PPP1R3C is involved in TORC2 dephosphorylation. Knockdown of PPP1R3C blocked cAMP-induced dephosphorylation of TORC2 and forskolin-promoted nucleus entry in mouse hepatocytes, but did not affect cAMP-stimulated CREB phosphorylation. CREB overexpression-elicited hepatic gluconeogenesis was attenuated by PPP1R3C silence. These results suggest that the unique effect of PP1 on target proteins is dependent on its regulatory unit. cAMP-stimulated PPP1R3C expression is involved in the enhancement of gluconeogenic programme *via* inducing TORC2 dephosphorylation, which could be disrupted by AMPK activation.

PPP1R3C, encoding protein targeting to glycogen (PTG), is a member of the family of glycogen-targeting subunits of protein phosphatase-1 [46]. It is widely accepted that PTG is a positive regulator of glycogen synthesis [46–48]. However, there exist contradictory results about its role in the regulation of whole-body glucose homeostasis. Overexpression of PTG in rat liver by adenoviral infection improved glucose tolerance, with increased hepatic glycogen accumulation [25]. PTG heterozygous knockout mice developed age-dependent glucose intolerance and insulin resistance, with a reduction of glycogen in multiple tissues [23]. However, a recent study showed that high-fat diet led to an increase in hepatic glycogen content *via* inducing PTG expression in the liver of mice. Homozygous deletion of PTG alleviated glucose intolerance and insulin resistance in high-fat diet-fed mice [49]. In the present study, hepatic Ppp1r3c mRNA expression in diabetic *db*/*db* mice was increased compared with that in control mice, suggesting that the abnormally high expression of Ppp1r3c in livers may be one of the main causes of hyperglycemia in diabetes. Enforced expression of PPP1R3C increased hepatic glucose production with elevated expressions of key gluconeogenic genes in normal wild-type mice. Conversely, Silence of

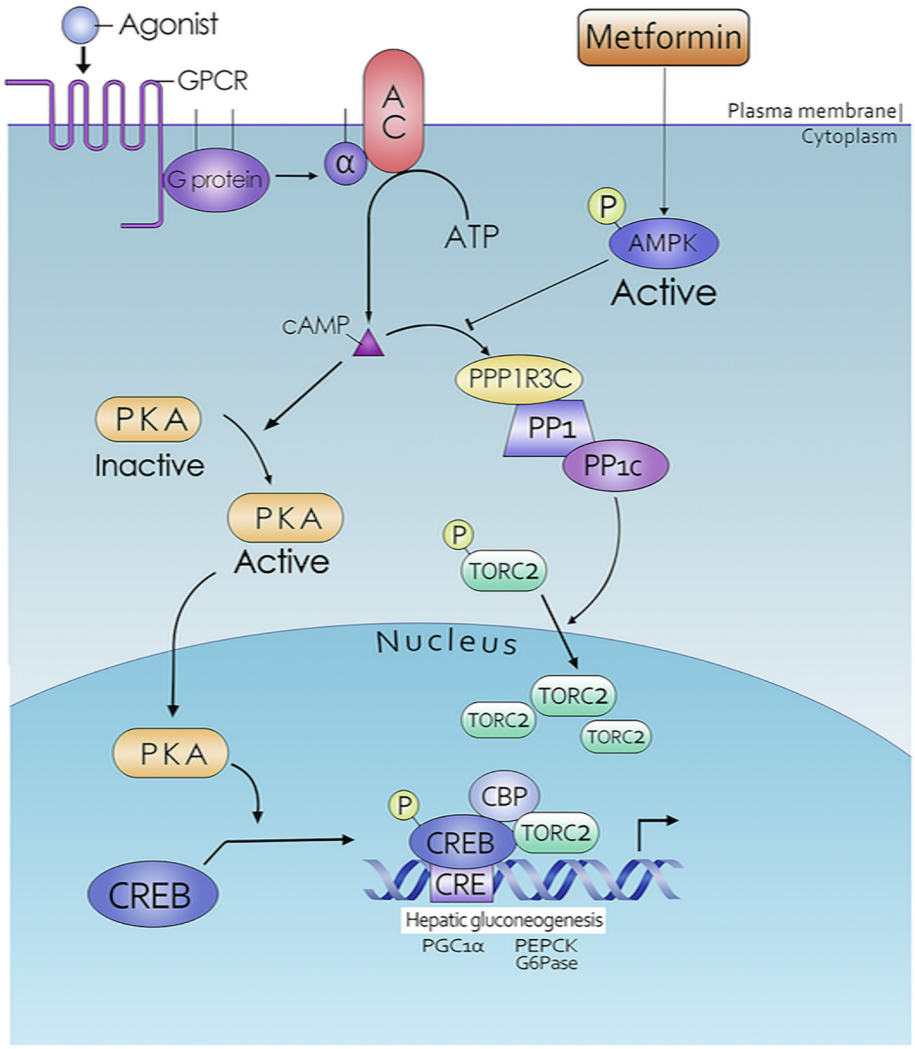

Fig. 8. Role of PPP1R3C in metformin-mediated inhibition of hepatic gluconeogenesis. During fasting status, raised intracellular cAMP increases the activity of PP1 *via* inducing PPP1R3C expression, leading to the dephosphorylation and nuclear entry of TORC2. In addition, cAMP stimulates PKA-mediated phosphorylation of CREB. The subsequent recruitment of CBP leads to the formation of a CREB-CBP-TORC2 complex, which triggers the transcription of hepatic gluconeogenic genes. Metformin suppresses cAMP-stimulated PPP1R3C expression *via* activating AMPK, blocking the dephosphorylation and nuclear entry of TORC2 and gluconeogenic process.

PPP1R3C decreased hepatic glucose production and glycogen accumulation with the downregulation of gluconeogenic gene expressions in normal wild-type mice as well as in *db*/*db* mice.

It has been demonstrated that hepatic glycogen synthesis is closely linked to the gluconeogenic process. In addition to glucose uptake, hepatic gluconeogenic fluxes determine the amount of glycogen formed, especially during fasting status [50]. It was reported that metformin inhibited both hepatic gluconeogenesis and glycogen synthesis, leading to a net decrease in endogenous glucose production and improved blood glucose level [51]. Other studies also showed that postprandial glycogen synthesis was inhibited if the gluconeogenic flux is blocked [52,53]. Overexpression of PPP1R3C in liver stimulates glycogen synthesis mainly from gluconeogenic precursors *via* the indirect pathway [25]. Consistent with this result, our *in vitro* and *in vivo* studies revealed that glycogen content was decreased in PPP1R3C silencing mice after hepatic gluconeogenesis was suppressed, which explains the effect of metformin on hepatic gluconeogenesis and glycogen synthesis. Our study suggests that PPP1R3C overexpression-stimulated gluconeogenesis provides glucose as a substrate for glycogen synthesis. PPP1R3C knockdown-suppressed gluconeogenesis contributes, at least in part, to less hepatic glycogen accumulation due to the short of substrates.

5. Conclusion

In summary, metformin treatment antagonizes cAMP-stimulated hepatic PPP1R3C expression *via* an AMPK-dependent pathway. Silence of PPP1R3C suppresses hepatic glucose production *via* blocking cAMP-induced dephosphorylation of TORC2 and expressions of key gluconeogenic enzymes and transcript factors (Fig. 8). In wild-type and *db*/*db* mice, hepatic knockdown of PPP1R3C decreases blood glucose level and improves pyruvate tolerance. PPP1R3C is a molecule linking hepatic gluconeogenesis to glycogen synthesis. Therefore, liver-specific knockout of PPP1R3C will provide a new strategy for the treatment of type 2 diabetes.

Declaration of Competing Interest

Authors have no conflict of interest.

Acknowledgements and funding

This work was supported by the National Natural Science Foundation of China (grant numbers 81471030, 81570693, 81770767, and 81870526).

Author contributions

XJ, SW, HT and YZ performed experiments. XJ, SW, HT and FZ analyzed the data. FZ, QZ, KZ, QL and Y.L. assisted with experiments. XJ, HT, XW and LZ conceived and designed the project. XJ, SW, XW and LZ wrote the manuscript. XW and LZ obtained funding and directed the study. All authors edited and reviewed the final manuscript.

Appendix A. Supplementary data

Supplementary data to this article can be found online at https://doi.org/10.1016/j.metabol.2019.06.002.

References

[1] Kahn SE, Cooper ME, Del Prato S. Pathophysiology and treatment of type 2 diabetes: perspectives on the past, present, and future. Lancet 2014;383:1068–83. https://doi.org/10.1016/S0140-6736(13)62154-6.

[2] Tan YZ, Cheen MHH, Goh SY, Bee YM, Lim PS, Khee GY, et al. Trends in medication utilization, glycemic control and outcomes among type 2 diabetes patients in a tertiary referral centre in Singapore from 2007 to 2017. J Diabetes 2018, Dec 16. https://doi.org/10.1111/1753-0407.12886.

[3] Hundal RS, Krssak M, Dufour S, Laurent D, Lebon V, Chandramouli V, et al. Mechanism by which metformin reduces glucose production in type 2 diabetes. Diabetes 2000;49:2063–9. https://doi.org/10.2337/diabetes.49.12.2063.

[4] Shaw RJ, Lamia KA, Vasquez D, Koo SH, Bardeesy N, Depinho RA, et al. The kinase LKB1 mediates glucose homeostasis in liver and therapeutic effects of metformin. Science 2005;310:1642–6. https://doi.org/10.1126/science.1120781.

[5] Jiang G, Zhang BB. Glucagon and regulation of glucose metabolism. Am J Physiol Endocrinol Metab 2003;284:E671–8. https://doi.org/10.1152/ajpendo.00492.2002.

[6] Unger RH, Cherrington AD. Glucagonocentric restructuring of diabetes: a pathophysiologic and therapeutic makeover. J Clin Invest 2012;122:4–12. https://doi.org/10.1172/JCI60016.

[7] Miller RA, Chu Q, Xie J, Foretz M, Viollet B, Birnbaum MJ. Biguanides suppress hepatic glucagon signalling by decreasing production of cyclic AMP. Nature 2013;494:256–60. https://doi.org/10.1038/nature11808.

[8] Hawley SA, Gadalla AE, Olsen GS, Hardie DG. The antidiabetic drug metformin activates the AMP-activated protein kinase cascade via an adenine nucleotide-independent mechanism. Diabetes 2002;51:2420–5. https://doi.org/10.2337/diabetes.51.8.2420.

[9] Hardie DG, Hawley SA, Scott JW. AMP-activated protein kinase—development of the energy sensor concept. J Physiol 2006;574:7–15. https://doi.org/10.1113/jphysiol.2006.108944.

[10] Zhou G, Myers R, Li Y, Chen Y, Shen X, Fenyk-Melody J, et al. Role of AMP-activated protein kinase in mechanism of metformin action. J Clin Invest 2001;108:1167–74. https://doi.org/10.1172/JCI13505.

[11] Lochhead PA, Salt IP, Walker KS, Hardie DG, Sutherland C. 5-aminoimidazole-4-carboxamide riboside mimics the effects of insulin on the expression of the 2 key gluconeogenic genes PEPCK and glucose-6-phosphatase. Diabetes 2000;49:896–903. https://doi.org/10.2337/diabetes.49.6.896.

[12] Cool B, Zinker B, Chiou W, Kifle L, Cao N, Perham M, et al. Identification and characterization of a small molecule AMPK activator that treats key components of type 2 diabetes and the metabolic syndrome. Cell Metab 2006;3:403–16. https://doi.org/10.1016/j.cmet.2006.05.005.

[13] Foretz M, Hebrard S, Leclerc J, Zarrinpashneh E, Soty M, Mithieux G, et al. Metformin inhibits hepatic gluconeogenesis in mice independently of the LKB1/AMPK pathway via a decrease in hepatic energy state. J Clin Invest 2010;120:2355–69. https://doi.org/10.1172/JCI40671.

[14] Ravnskjaer K, Kester H, Liu Y, Zhang X, Lee D, Yates 3rd JR, et al. Cooperative interactions between CBP and TORC2 confer selectivity to CREB target gene expression. EMBO J 2007;26:2880–9. https://doi.org/10.1038/sj.emboj.7601715.

[15] Xu W, Kasper LH, Lerach S, Jeevan T, Brindle PK. Individual CREB-target genes dictate usage of distinct cAMP-responsive coactivation mechanisms. EMBO J 2007;26:2890–903. https://doi.org/10.1038/sj.emboj.7601734.

[16] Chrivia JC, Kwok RP, Lamb N, Hagiwara M, Montminy MR, Goodman RH. Phosphorylated CREB binds specifically to the nuclear protein CBP. Nature 1993;365:855–9. https://doi.org/10.1038/365855a0.

[17] Koo SH, Flechner L, Qi L, Zhang X, Screaton RA, Jeffries S, et al. The CREB coactivator TORC2 is a key regulator of fasting glucose metabolism. Nature 2005;437:1109–11. https://doi.org/10.1038/nature03967.

[18] Han HS, Choi BH, Kim JS, Kang G, Koo SH. Hepatic Crtc2 controls whole body energy metabolism via a miR-34a-Fgf21 axis. Nat Commun 2017;8:1878. https://doi.org/10.1038/s41467-017-01878-6.

[19] Cohen PT. Protein phosphatase 1—targeted in many directions. J Cell Sci 2002;115:241–56.

[20] Zhang T, Wang S, Lin Y, Xu W, Ye D, Xiong Y, et al. Acetylation negatively regulates glycogen phosphorylase by recruiting protein phosphatase 1. Cell Metab 2012;15:75–87. https://doi.org/10.1016/j.cmet.2011.12.005.

[21] Alemany S, Cohen P. Phosphorylase a is an allosteric inhibitor of the glycogen and microsomal forms of rat hepatic protein phosphatase-1. FEBS Lett 1986;198:194–202. https://doi.org/10.1016/0014-5793(86)80404-5.

[22] Berman HK, O'Doherty RM, Anderson P, Newgard CB. Overexpression of protein targeting to glycogen (PTG) in rat hepatocytes causes profound activation of glycogen synthesis independent of normal hormone- and substrate-mediated regulatory mechanisms. J Biol Chem 1998;273:26421–5. https://doi.org/10.1074/jbc.273.41.26421.

[23] Crosson SM, Khan A, Printen J, Pessin JE, Saltiel AR. PTG gene deletion causes impaired glycogen synthesis and developmental insulin resistance. J Clin Invest 2003;111:1423–32. https://doi.org/10.1172/JCI17975.

[24] Subramanian A, Tamayo P, Mootha VK, Mukherjee S, Ebert BL, Gillette MA, et al. Gene set enrichment analysis: a knowledge-based approach for interpreting genome-wide expression profiles. Proc Natl Acad Sci U S A 2005;102:15545–50. https://doi.org/10.1073/pnas.0506580102.

[25] O'Doherty RM, Jensen PB, Anderson P, Jones JG, Berman HK, Kearney D, et al. Activation of direct and indirect pathways of glycogen synthesis by hepatic overexpression of protein targeting to glycogen. J Clin Invest 2000;105:479–88. https://doi.org/10.1172/JCI8673.

[26] Brady MJ, Printen JA, Mastick CC, Saltiel AR. Role of protein targeting to glycogen (PTG) in the regulation of protein phosphatase-1 activity. J Biol Chem 1997;272:20198–204. https://doi.org/10.1016/j.mam.2015.09.002.

[27] Screaton RA, Conkright MD, Katoh Y, Best JL, Canettieri G, Jeffries S, et al. The CREB coactivator TORC2 functions as a calcium- and cAMP-sensitive coincidence detector. Cell 2004;119:61–74. https://doi.org/10.1016/j.cell.2004.09.015.

[28] Petersen MC, Vatner DF, Shulman GI. Regulation of hepatic glucose metabolism in health and disease. Nat Rev Endocrinol 2017;13:572–87. https://doi.org/10.1038/nrendo.2017.80.

[29] Magnusson I, Rothman DL, Katz LD, Shulman RG, Shulman GI. Increased rate of gluconeogenesis in type II diabetes mellitus. A 13C nuclear magnetic resonance study. J Clin Invest 1992;90:1323–7. https://doi.org/10.1172/JCI115997.

[30] Viollet B, Guigas B, Sanz Garcia N, Leclerc J, Foretz M, Andreelli F. Cellular and molecular mechanisms of metformin: an overview. Clin Sci (Lond) 2012;122:253–70. https://doi.org/10.1042/CS20110386.

[31] Stephenne X, Foretz M, Taleux N, van der Zon GC, Sokal E, Hue L, et al. Metformin activates AMP-activated protein kinase in primary human hepatocytes by decreasing cellular energy status. Diabetologia 2011;54:3101–10. https://doi.org/10.1007/s00125-011-2311-5.

[32] Suter M, Riek U, Tuerk R, Schlattner U, Wallimann T, Neumann D. Dissecting the role of 5'-AMP for allosteric stimulation, activation, and deactivation of AMP-activated protein kinase. J Biol Chem 2006;281:32207–16. https://doi.org/10.1074/jbc.M606357200.

[33] Cao J, Meng S, Chang E, Beckwith-Fickas K, Xiong L, Cole RN, et al. Low concentrations of metformin suppress glucose production in hepatocytes through AMP-activated protein kinase (AMPK). J Biol Chem 2014;289:20435–46. https://doi.org/10.1074/jbc.M114.604421.

[34] Altarejos JY, Montminy M. CREB and the CRTC co-activators: sensors for hormonal and metabolic signals. Nat Rev Mol Cell Biol 2011;12:141–51. https://doi.org/10.1038/nrm3072.

[35] Dentin R, Liu Y, Koo SH, Hedrick S, Vargas T, Heredia J, et al. Insulin modulates gluconeogenesis by inhibition of the coactivator TORC2. Nature 2007;449:366–9. https://doi.org/10.1038/nature06128.

[36] Iourgenko V, Zhang W, Mickanin C, Daly I, Jiang C, Hexham JM, et al. Identification of a family of cAMP response element-binding protein coactivators by genome-scale functional analysis in mammalian cells. Proc Natl Acad Sci U S A 2003;100:12147–52. https://doi.org/10.1073/pnas.1932773100.

[37] Allaman I, Pellerin L, Magistretti PJ. Protein targeting to glycogen mRNA expression is stimulated by noradrenaline in mouse cortical astrocytes. Glia 2000;30:382–91. https://doi.org/10.1002/(sici)1098-1136(200006)30:4<382::aid-glia70>3.0.co;2-0.

[38] Zhang LP, Rubins NE, Ahima RS, Greenbaum LE, Kaestner KH. Foxa2 integrates the transcriptional response of the hepatocyte to fasting. Cell Metab 2005;2:141–8. https://doi.org/10.1016/j.cmet.2005.07.002.

[39] Cheng A, Zhang M, Crosson SM, Bao ZQ, Saltiel AR. Regulation of the mouse protein targeting to glycogen (PTG) promoter by the FoxA2 forkhead protein and by 3′,5′-cyclic adenosine 5′-monophosphate in H4IIE hepatoma cells. Endocrinology 2006;147:3606–12. https://doi.org/10.1210/en.2005-1513.

[40] Kim YD, Park KG, Lee YS, Park YY, Kim DK, Nedumaran B, et al. Metformin inhibits hepatic gluconeogenesis through AMP-activated protein kinase-dependent regulation of the orphan nuclear receptor SHP. Diabetes 2008;57:306–14. https://doi.org/10.2337/db07-0381.

[41] Johanns M, Lai YC, Hsu MF, Jacobs R, Vertommen D, Van Sande J, et al. AMPK antagonizes hepatic glucagon-stimulated cyclic AMP signalling via phosphorylation-induced activation of cyclic nucleotide phosphodiesterase 4B. Nat Commun 2016;7:10856. https://doi.org/10.1038/ncomms10856.

[42] Wadzinski BE, Wheat WH, Jaspers S, Peruski Jr LF, Lickteig RL, Johnson GL, et al. Nuclear protein phosphatase 2A dephosphorylates protein kinase A-phosphorylated CREB and regulates CREB transcriptional stimulation. Mol Cell Biol 1993;13:2822–34. https://doi.org/10.1128/mcb.14.9.5881.

[43] Wang Y, Inoue H, Ravnskjaer K. Targeted disruption of the CREB coactivator Crtc2 increases insulin sensitivity. Proc Natl Acad Sci U S A 2010;107:3087–92. https://doi.org/10.1073/pnas.0914897107.

[44] Yoon YS, Lee MW, Ryu D. Suppressor of MEK null (SMEK)/protein phosphatase 4 catalytic subunit (PP4C) is a key regulator of hepatic gluconeogenesis. Proc Natl Acad Sci U S A 2010;107:17704–9. https://doi.org/10.1073/pnas.1012665107.

[45] Uebi T, Tamura M, Horike N, Hashimoto YK, Takemori H. Phosphorylation of the CREB-specific coactivator TORC2 at Ser(307) regulates its intracellular localization in COS-7 cells and in the mouse liver. Am J Physiol Endocrinol Metab 2010;299:E413–25. https://doi.org/10.1152/ajpendo.00525.2009.

[46] Printen JA, Brady MJ, Saltiel AR. PTG, a protein phosphatase 1-binding protein with a role in glycogen metabolism. Science 1997;275:1475–8. https://doi.org/10.1126/science.275.5305.1475.
[47] Greenberg CC, Meredith KN, Yan L, Brady MJ. Protein targeting to glycogen overexpression results in the specific enhancement of glycogen storage in 3T3-L1 adipocytes. J Biol Chem 2003;278:30835–42. https://doi.org/10.1074/jbc.M303846200.
[48] Greenberg CC, Danos AM, Brady MJ. Central role for protein targeting to glycogen in the maintenance of cellular glycogen stores in 3T3-L1 adipocytes. Mol Cell Biol 2006;26:334–42. https://doi.org/10.1128/MCB.26.1.334-342.2006.
[49] Lu B, Bridges D, Yang Y, Fisher K, Cheng A, Chang L, et al. Metabolic crosstalk: molecular links between glycogen and lipid metabolism in obesity. Diabetes 2014;63:2935–48. https://doi.org/10.2337/db13-1531.
[50] Radziuk J, Pye S. Hepatic glucose uptake, gluconeogenesis and the regulation of glycogen synthesis. Diabetes Metab Res Rev 2001;17:250–72.
[51] Radziuk J, Zhang Z, Wiernsperger N, Pye S. Effects of metformin on lactate uptake and gluconeogenesis in the perfused rat liver. Diabetes 1997;46:1406–13.
[52] Sugden MC, Watts DI, Palmer TN, Myles DD. Direction of carbon flux in starvation and after refeeding: in vitro and in vivo effects of 3-mercaptopicolinate. Biochem Int 1983;7:329–37.
[53] Newgard CB, Moore SV, Foster DW, McGarry JD. Efficient hepatic glycogen synthesis in refeeding rats requires continued carbon flow through the gluconeogenic pathway. J Biol Chem 1984;259:6958–63.